Actinides

DOI: 10.1002/anie.200906129

Solving the Hydration Structure of the Heaviest Actinide Aqua Ion Known: The Californium(III) Case**

Elsa Galbis, Jorge Hernández-Cobos, Christophe den Auwer, Claire Le Naour, Dominique Guillaumont, Eric Simoni, Rafael R. Pappalardo, and Enrique Sánchez Marcos**

The solution chemistry of actinide ions has been a fundamental question since the beginning of the nuclear technologies, given that the solvent stabilizes the high oxidation states of actinides.[1] The development of procedures to avoid the migration of actinides from the already accumulated nuclear waste into natural water systems is a field of great activity.[2] One of the primary properties of actinide ions in solution is their solvation, as it is intimately joined to complexation, precipitation, and resolution processes. The rareness and hazardousness of the heavier actinide elements, which steeply increase with the atomic number, has prevented a complete examination of the trends along the series, beyond the middle of the series.[3] The curium cation Cm^{III} has often been considered as the heaviest actinide species characterized, and it has attracted much attention from both experimental and theoretical views in recent years.[3,4] Systematic studies of the aqueous trivalent lanthanides have revealed a contraction of the metal–oxygen distance and a decrease of the total first coordination number along the series.[5] Recent investigations using extended X-ray absorption fine structure (EXAFS) techniques have examined if this contraction takes place in a monotone or an irregular way along the series.[6] The data available for the actinide series up to Cm^{III} indicates a similar contraction,[3,5,7] although a conclusive answer cannot be given owing to the uncertainty of the structural data, particularly concerning the hydration number, and the scarce information on the second half of the series. Beyond the middle of the series, there is only one study reported for berkelium (Bk^{III})[8] and a preliminary EXAFS study for californium(III) carried out by one of us.[9] Owing to the position of Cf^{III} in the actinide series, an accurate enough determination of the coordination number and Cf–O distance could certainly shed light on the question of the actinide contraction. This objective gives the study a more fundamental than applied character, owing to the extreme rareness of this element. The most similar available crystallographic data of Cf^{III} with Cf–O bonds is that of single crystals of $Cf(IO_3)_3$, which present a significantly distorted tricapped trigonal prism with a wide range of Cf–O distances (2.353–2.921 Å).[10] This limited information does not meet the required level of accuracy for answering the question on the basis of a conventional EXAFS data analysis.

Herein we present an alternative way to study this extreme case, by coupling new highly refined EXAFS data obtained in an actinide-dedicated beamline in the European Synchrotron Radiation Facility (ESRF, Grenoble), with the first Monte Carlo (MC) simulations of Cf^{III} in water. Specifically developed Cf–OH_2 intermolecular potentials based on ab initio quantum mechanical (QM) potential energy surfaces and the polarizable and flexible MCDHO water model[11] have been used.

Figure 1 shows the experimental and fitted k^2-weighted EXAFS spectra of a Cf^{III} aqueous solution using two model structures, the square antiprism configuration (SA; see Figure 2a), which represents an octacoordination of water

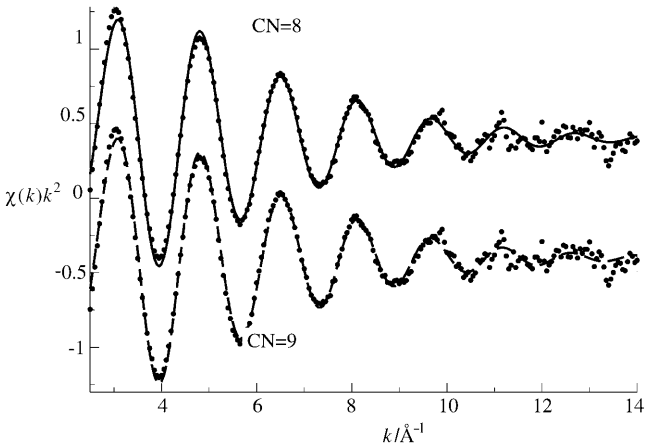

Figure 1. Experimental (black points) and fitted (solid and dashed lines) Cf L_{III}-edge EXAFS spectrum of Cf^{III} aqueous solution, using as aqua ion models the square antiprism (CN = 8, top) and the trigonal tricapped prism (CN = 9, bottom).

[*] E. Galbis, Dr. R. R. Pappalardo, Prof. E. Sánchez Marcos
Departamento de Química Física, Universidad de Sevilla
41012 Sevilla (Spain)
Fax: (+34) 95-455-7174
E-mail: sanchez@us.es
Dr. J. Hernández-Cobos
Instituto de Ciencias Físicas
Apartado Postal 48-3, 62251 Cuernavaca (México)
Dr. C. den Auwer, Dr. D. Guillaumont
CEA, Nuclear Energy Division
Radiochemistry Process Department, SCPS/LILA
30207 Bagnols sur Cèze (France)
E-mail: christophe.denauwer@cea.fr
Dr. C. Le Naour, Prof. E. Simoni
Institut de Physique Nucleaire Orsay, Université Paris-Sud (France)

[**] Junta de Andalucia (Project number P06-FQM-01484) is acknowledged for financial support. ESRF and FZDR are acknowledged for beamtime allocation at the BM20/ROBL beamline. We are indebted for the loan of ^{249}Cf through the US Department of Energy via the High Flux Isotope Reactor and Radioelement Development Centre of Oak Ridge NL.

Supporting information for this article is available on the WWW under http://dx.doi.org/10.1002/anie.200906129.

© 2010 Wiley-VCH Verlag GmbH & Co. KGaA, Weinheim

molecules, and the trigonal tricapped prism (TTP) (see Figure 2c) which implies an enneacoordination. Experimental details on sample preparation and EXAFS data acquisition and processing are given in the Supporting Information. As no experimental estimation of the global amplitude factor S_o^2 can be obtained for the californium case, during the fitting procedure the coordination numbers were fixed to the model values of eight and nine, respectively. Best-fit EXAFS parameters derived from both models are collected in Table 1. There is no clearly visible difference between the

Table 1: Best-fit parameters (Cf–O distance, Debye–Waller factors, and $\Re$ factor of the fit) for the Cf L_{III}-edge EXAFS spectrum using as aqua ion model either the square antiprism (SA) polyhedron or the trigonal tricapped prism (TTP).

Model	R_{Cf-O} [Å]	σ^2 [Å^2]	$\Re$
SA (CN = 8)[a]	2.42(1)	0.0077	1.9
TTP (CN = 9)[b]	2.38(1) × 6	0.0068	1.9
	2.47(1) × 3	0.0039	

[a] $S_o^2 = 0.9$, $E_o = 1.76$ eV, $\varepsilon = 0.0033$, $\Delta\chi^2_v = 0.2$. [b] $S_o^2 = 0.9$, $E_o = 1.76$ eV, $\varepsilon = 0.0033$, $\Delta\chi^2_v = 0.2$. E_o = inner potential correction, ε = spectrum noise, $\Delta\chi^2_v$ = quality factor.

two fitted curves, and none of the adjusted parameters in Table 1 allow the rejection of one of the two structural models. Furthermore, the weighted averages of the Cf–O distances are comparable: eight oxygen atoms at 2.42 Å for SA, nine oxygen atoms at 2.41 Å for TTP, keeping in mind that a difference of one unit in coordination number over nine (11%) is not significant from the EXAFS point of view, especially in the absence of experimental S_0^2 values. The fitted value of S_0^2 is 0.9, which is equal to the value obtained for a plutonium(III) aqueous solution recorded at the same beamline[12] and similar to the S_0^2 value of 1.0 employed by Soderhlom et al. in the Cm^{III} case.[3a] The model of a uniform enneacoordination leads to fitting results quite close to those obtained for the SA model, showing a similar Cf–O distance, but with its associated Debye–Waller (DW) factor (σ^2) slightly higher and the S_o^2 value slightly smaller than for the octahydrate model. The σ^2 value for the SA model (0.0077 Å^2) is higher than those of the TTP configuration and the two sets of Cf–O distances in the enneahydrate. This result could suggest a significant distortion of the hydration shell in the SA configuration. Indeed, Debye–Waller factors for both TTP shells are significantly lower (0.0039 and 0.0068 Å^2). These results also indicate that the three capping oxygen atoms are less disordered than the six prismatic ones. For the Cm^{III} case, Skanthakumar et al. give a value for the SA model (0.0071 Å^2),[3a] whereas the relative values for the DW factors corresponding to the two different Cm–O distances were exchanged with respect to the Cf^{III} case when the TTP model was employed.[3] In two recent related papers on the crystal and aqueous structures of lanthanide(III) aqua ions,[6] the samarium(III) case shows similar DW factor distributions to the Cf^{III} one, whereas others cations such as lanthanum(III) and dysprosium(III) are more similar to the Cm^{III} case. In the present study, attempts to force the same relative values for the Debye–Waller factors in the TTP model always led to significantly degraded fits. Contrary to what is observed for Cm^{III} and Ln^{III} in aqueous solution, distinction between a TTP and a SA configuration cannot be unambiguously deduced from the fittings.

Computer simulation of Cf^{III} in water represents a completely independent approach to the study of this system. However, no intermolecular Cf^{III}–OH_2 potential has been proposed in the literature to carry out classical computer simulations, nor have ab initio molecular dynamics (MD) simulations been carried out. Herein, we have developed two independent Cf–OH_2 intermolecular potentials based on ab initio potential energy surfaces. We have taken advantage of the QM methodology developed by Dolg and co-workers[13a] for the trivalent actinides. They used the MP2 level and DFT by applying the BP86 functional in the QM study of the $[An(H_2O)_n]^{3+}$ series for $n = 7$, 8, and 9. A set of quasi-relativistic An^{III} 5f-core pseudopotentials were specifically developed for this objective.[13b] These authors included the solvent effects on the possible aqua ions by means of the PCM continuum model. They conclude that the hydration number must range between eight and nine water molecules for the An^{III} ions. We use these two different QM models, as according to Dolg and co-workers' study[13a] the BP86 method favors the octacoordination, whereas the MP2 method favors higher coordination close to nine. In this way, the two computer simulations derived from them may represent a reasonable range of the Cf^{III} hydration number.

The model of Cf–OH_2 intermolecular potential has been inspired by the hydrated ion concept, which has demonstrated its good performance in the computer simulation of other highly charged metal cations.[14] In its original formulation, the model assumes a high stability of the hydrated ion, such that the exchange of water molecules between the first and the second hydration shell is prevented. Although this assumption is valid for cations such as chromium(III) or iridium(III), it no longer holds true for large cations, such as actinides or lanthanides. Thus, to improve our original hydrated ion model, a polarizable and flexible water model, the MCDHO model,[11] has been adopted, and the Cf^{III} ion has also been described as a polarizable particle. The intermolecular Cf^{III}–OH_2 potential was extracted from the potential energy surfaces formed by one cation and a variable set of water molecules, $[Cf(H_2O)_n]^{3+}$ ($7 \le n \le 9$), by scanning the release of a water molecule from the closest environment of the cation in the presence of the rest of first-shell water molecules at the BP86 and MP2 levels. Figure 2 shows the BP86 optimized structures for the octa- and enneahydrate (Figure 2a,c) as well as structures corresponding to the scans releasing a water molecule from the octahydrate (Figure 2b) or the enneahydrate (Figure 2d).

The QM global formation energy ΔE_{form} of the $[Cf(H_2O)_n]^{3+}$ cluster is decomposed into the different contributions of the molecules involved in the cluster and fitted to a pair potential U_{inter} [Eq. (1)]:

$$\Delta E_{form} = E_{[Cf(H_2O)_n]^{3+}} - E_{Cf^{3+}} - nE_{H_2O} = U_{inter} = \sum_{i=1}^{N}\sum_{j>i}^{N} U_{ij}(r_{ij})$$

 © 2010 Wiley-VCH Verlag GmbH & Co. KGaA, Weinheim

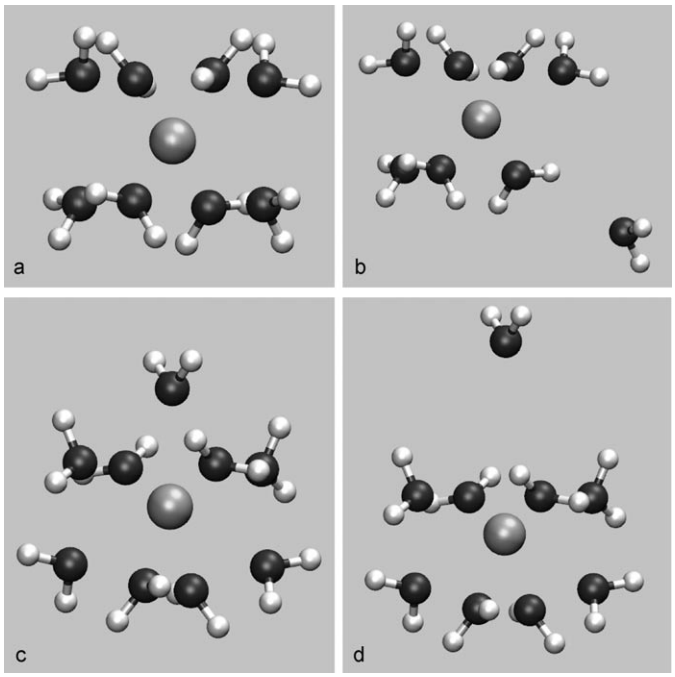

Figure 2. Some structures used for the construction of the Cf^{III}–OH_2 intermolecular potential: a, c) BP86 optimized geometries for the octahydrate and enneahydrate, respectively. b, d) Distorted structures in which one of the water molecules is released from its equilibrium position.

where the polarizable character of the californium ion and the water molecule, in addition to the flexible character of the water molecule, allow an individual nuclear and charge distribution relaxation of every molecule of the cluster, although the fitted coefficients of the $U_{ij}(r_{ij})$ are common. This method of building the intermolecular potential collects to a large extent the many-body interactions up to roughly the ninth order, particularly in the first hydration shell, where these interactions are more important than in the outer shells.[14] The flexible and polarizable character of the water model allows a proper tuning of the strong polarization changes suffered by the water molecule when going from the first to outer hydration shells. Details about the construction of this new type of potential and the Monte Carlo (MC) simulations are given in the Supporting Information. The two new potentials have been tested by comparing their results with the QM results of the octahydrate and enneahydrate aqua ions, as well as their hydrated forms, $[Cf(H_2O)_8]^{3+}\cdot(H_2O)_{16}$ and $[Cf(H_2O)_9]^{3+}\cdot(H_2O)_{18}$. In the Supporting Information, the ΔE_{form} values (Table S1) and the optimized structures (Figure S1) are compared. Both sets of results support the good behavior of the potentials and their energy gradients.

MC simulations for a system formed by $1\,Cf^{III} + 500\,H_2O$ at 300 K in the canonical ensemble (NVT) were carried out. Structures for analysis were taken from a statistical sampling of 2×10^9 configurations. The MC simulation using the Cf–OH_2 potential derived from the BP86 potential energy surface (BP86 simulation) leads to an average coordination number for the first coordination shell close to 8 (7.5), and the first maximum of the Cf–O radial distribution function (RDF) appears at 2.43 Å, whereas the MC simulation which uses the Cf–OH_2 potential derived from the MP2 potential energy surface (MP2 simulation) gives a hydration number close to 9 (8.8), and the maximum for the Cf–O RDF appears at 2.53 Å. These general trends are in agreement with the QM study of An^{III} aqua ions recently reported by Dolg and coworkers.[13a] The second coordination shell is formed by 16–17 (BP86 simulation) and 18–19 (MP2 simulation) water molecules centered at 4.65 and 4.69 Å, respectively. The absence of experimental properties other than the EXAFS spectrum which could be compared with the predicted value derived from the statistical model precludes the adoption of a convincing criterion to clearly select one intermolecular potential with respect to the other.

The third step in this study is to combine the experimental and the theoretical results. The question to answer is which simulation provides a better agreement with the experimental results, and consequently which is the hydration number. The computation of X-ray absorption spectra from the structural information provided by computer simulations has proven a powerful tool for solving delicate structural problems such as the determination of the second shell.[15] 2000 configurations from each MC simulation have been selected to compute individually the Cf L_{III}-edge EXAFS spectra applying the FEFF code (version 8.4).[16] A scheme of the procedure is given in Figure S2 in the Supporting Information. Different cutoff radii ($R_{cut} = 3.5$–5.5 Å) have been employed to examine the number of hydration shells affecting the EXAFS signal. This study has determined that the second hydration shell has a marginal influence on the final computed spectrum. This finding is contrary to the cases of lighter trivalent cations such as Cr^{III}[15b] or Ir^{III},[15d] for which the high stability of the first shell allows a robust second hydration shell to be maintained that indeed contributes to the backscattering signal. For the Cf^{III} structure, as already reported for other lanthanide[17] and actinide[4d] cations, the water exchange and high fluxionality of the first shell preclude a stable enough second shell to contribute to the backscattering signal significantly. The k^2-weighted EXAFS spectra averaged over all structures taken from the BP86 and MP2 simulations are plotted in Figure 3 and compared with the experimental spectrum. The only parameter of the simulated spectra which was fitted with respect to the experimental one was the value employed for E_o, chosen to best phase the computed signal with the experimental data. The agreement between simulated and experimental spectra is remarkable for the case of the BP86 simulation, where the intensity of the signal and the in-phase behavior is maintained up to the point at which the experimental spectrum is blurred by the high noise/signal ratio. For the case of the MP2 simulation, the computed spectrum shows an intensity less similar to the experimental one and a progressive out-of-phase behavior owing to the higher frequency of the computed EXAFS oscillations. Bearing in mind that the first computed spectrum is derived from the BP86 MC simulation, for which $n \approx 8$ and $R_{Cf-O} =$ 2.43 Å, whereas the second computed spectrum comes from the MP2 MC simulation, for which $n \approx 9$ and $R_{Cf-O} = 2.53$ Å,

 © 2010 Wiley-VCH Verlag GmbH & Co. KGaA, Weinheim

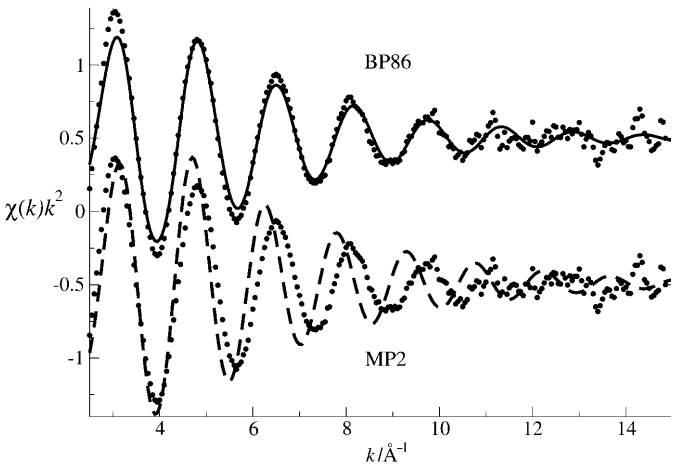

Figure 3. Comparison of the k^2-weighted Cf L_{III}-edge EXAFS spectrum of a 1 mM Cf^{III} aqueous solution in perchloric acid (black points) with the computed spectra obtained from the set of snapshots of the MC BP86 (top) or MP2 (bottom) simulation.

we must conclude that the Cf^{III} aqua ion is mainly octacoordinated and its average mean Cf–O distance is around 2.43 Å.

Additional analysis can be done to gain insight into the factors determining the ability of the methodology to reproduce the experimental EXAFS spectrum. The first is the exploration of the influence of the QM level employed, and the second is the role of the statistical sampling. Four EXAFS spectra using only one structure of the Cf^{III} aqua ion have been computed, instead of averaging on a wide set of statistically generated structures. The $[Cf(H_2O)_8]^{3+}$ and $[Cf(H_2O)_9]^{3+}$ optimized geometries at the MP2 and BP86 levels have been employed (A scheme of the procedure is given in Figure S2 in the Supporting Information). Figure 4 plots the four spectra together with the experimental one. The intensity of all the simulated spectra is much higher than that of the experimental one, contrary to what is observed for the computed spectra derived from the average of the statistical sampling (see Figure 3). This result is a consequence of the lack of a DW factor applied to these model structures. However, the spectra computed from the MC simulations show how the fluctuations of the near Cf^{III} environment supplied by the statistical average adequately represent the structural distortions of the aqua ions. In other words, the statistical average borne by the MP2 and BP86 simulations implicitly includes the DW factors, whereas the use of only one structure, even though it was the QM optimized one, is lacking the disorder accounted for by the DW factors. The second interesting conclusion derived from the analysis of Figure 4 with respect to Figure 3 is that the coordination number (solid line for CN = 8 and dashed line for CN = 9) is more important than the computational level (top for the BP86 optimized structures and bottom for the MP2 ones) in determining the phase. Joined to this structural fact is the relative value of the Cf–O distance, which is smaller for the octacoordinate hydrates ($R_{Cf-O} = 2.48$–2.49 Å) than for their enneacoordinate counterparts ($R_{Cf-O} = 2.51$–2.54 Å). There is not a clear preference for a given QM model. A third remark is that even for the eight-fold coordination, a phase shift of the computed spectra is found, whereas such a shift is not found in the statistically averaged BP86 EXAFS spectrum. This additional improvement in the BP86 statistically averaged spectrum indicates that beyond the included intrinsic disorder, which is responsible for the correct intensity of the signal, the average of single and multiple scattering contributions to the EXAFS spectrum subtly changes the phase of the signal as a function of the k value. Therefore, this result leads us to conclude that the elucidation of the hydration number based on the consideration of different rigid aqua ion models fails for highly dynamic aqua ions.

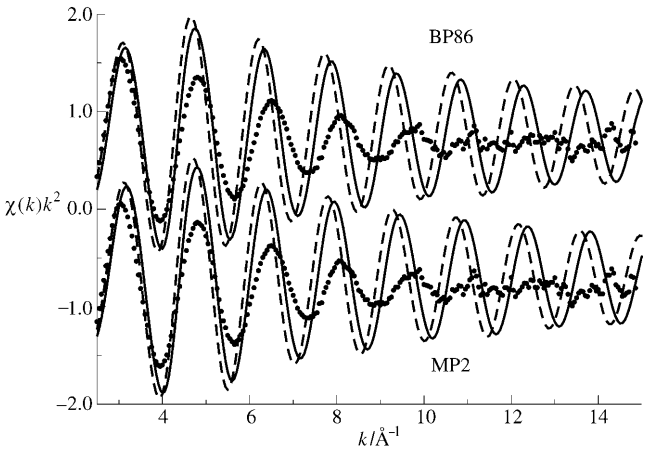

Figure 4. Comparison of the k^2-weighted Cf L_{III}-edge EXAFS spectrum of a 1 mM Cf^{III} aqueous solution in perchloric acid (black points) with the computed spectra obtained from the optimized MP2 (bottom) and BP86 (top) structures corresponding to the $[Cf(H_2O)_8]^{3+}$ (solid lines) and $[Cf(H_2O)_9]^{3+}$ (dashed lines) aqua ions.

In summary, the first MC simulation of the trivalent cation of californium, based on an exchangeable hydrated ion–water intermolecular potential, has been shown to extend and improve the hydrated ion model.[14] Likewise, the Cf L_{III}-edge EXAFS spectrum of an acidic 1 mM $Cf(ClO_4)_3$ aqueous solution recorded under optimized experimental conditions has greatly improved the signal/noise ratio of the only previously recorded spectrum.[9] The comparison of the experimental EXAFS spectrum with the two computed ones, obtained from two different intermolecular potentials that predict eight (BP86) or nine (MP2) water molecules in the first coordination shell, leads to the conclusion that the lowest hydration number is preferred. Then, as Cf^{III} is the heaviest actinide aqua ion for which there is experimental information, the actinide contraction is supported by the present study. (For U^{III}, $R_{U-O} = 2.56$ Å and $CN = 9 \pm 1$; for Pu^{III}, $R_{Pu-O} = 2.51$ Å and $CN = 9 \pm 1$; for Cm^{III}, $R_{Cm-O} = 2.47$ Å and $CN = 9 \pm 1$.)[3] The role of the second hydration shell is important in defining the structure and dynamics of the Cf^{III} aqua ion, but the contribution of second-shell water molecules to the EXAFS signal as backscatters is marginal.

Finally, this work gives an illustrative example of the benefits which can be achieved from the combination of experimental X-ray absorption spectroscopy and computer simulations. The usefulness of the simultaneous analysis of the results as well as the importance of the structural statistical average has been clearly demonstrated herein.

 © 2010 Wiley-VCH Verlag GmbH & Co. KGaA, Weinheim

Each technique independently was not adequate. We believe that this study traces out a still poorly explored combined methodology which may be extremely useful for many other complexes and chemical problems. A systematic theoretical and experimental examination of the other known actinide cations on the same basis should be undertaken to confirm the findings presented herein.

Received: October 30, 2009
Revised: March 12, 2010
Published online: April 16, 2010

Keywords: actinides · aqua ligands · computational chemistry · Monte Carlo simulation · X-ray spectroscopy

[1] R. J. Silva, H. Nitsche, *Radiochim. Acta* **1995**, *70–71*, 377 – 396.
[2] M. A. Denecke, *Coord. Chem. Rev.* **2006**, *250*, 730 – 754.
[3] a) S. Skanthakumar, M. R. Antonio, R. E. Wilson, L. Soderholm, *Inorg. Chem.* **2007**, *46*, 3485 – 3491; b) P. Lindqvist-Reis, C. Apostolidis, J. Rebizant, A. Morgenstern, R. Klenze, O. Walter, T. Fanghanel, R. G. Haire, *Angew. Chem. Int. Ed.* **2007**, *46*, 919 – 922; c) L. Soderholm, M. R. Antonio in *The Chemistry of the Actinide and Transactinide Elements*, *Vols. 4 and 5*, *3rd ed.* (Eds.:L. R. Moss, N. M. Edelstein, J. Fuger, J. J. Katz), Springer, Dordrecht, **2006**, pp. 3086 – 3198.
[4] a) T. Yang, B. E. Bursten, *Inorg. Chem.* **2006**, *45*, 5291 – 5301; b) N. M. Edelstein, R. Klenze, T. Fanghanel, S. Hubert, *Coord. Chem. Rev.* **2006**, *250*, 948 – 973; c) P. Lindqvist-Reis, C. Walther, R. Klenze, A. Eichhofer, T. Fanghanel, *J. Phys. Chem. B* **2006**, *110*, 5279 – 5285; d) D. Hagberg, E. Bednarz, N. M. Edelstein, L. Gagliardi, *J. Am. Chem. Soc.* **2007**, *129*, 14136 – 14137.
[5] a) T. Yamaguchi, M. Nomura, H. Wakita, H. Ohtaki, *J. Chem. Phys.* **1988**, *89*, 5153 – 5159; b) G. T. Seaborg, *Radiochim. Acta* **1993**, *61*, 115 – 122.
[6] a) I. Persson, P. D'Angelo, S. de Panfilis, M. Sandström, L. Eriksson, *Chem. Eur. J.* **2008**, *14*, 3056 – 3066; b) P. D'Angelo, S. de Panfilis, A. Filipponi, I. Persson, *Chem. Eur. J.* **2008**, *14*, 3045 – 3055.
[7] a) F. H. David, B. Fourest, *New J. Chem.* **1997**, *21*, 167 – 176; b) A. Bilewicz, *Radiochim. Acta* **2004**, *92*, 69 – 72; c) S. Cotton, *Lanthanides and Actinides Chemistry*, Wiley, New York, **2006**.
[8] M. R. Antonio, C. W. Williams, L. Soderholm, *Radiochim. Acta* **2002**, *90*, 851 – 856.
[9] R. Revel, C. Den Auwer, C. Madic, F. David, B. Fourest, S. Hubert, J.-F. Le Du, L. R. Morss, *Inorg. Chem.* **1999**, *38*, 4139 – 4141.
[10] R. E. Sykora, Z. Assefa, R. G. Haire, T. E. Albrecht-Schmitt, *Inorg. Chem.* **2006**, *45*, 475 – 477.
[11] H. Saint-Martin, J. Hernández-Cobos, M. I. Bernal-Uruchurtu, I. Ortega-Blake, J. C. Berendsen, *J. Chem. Phys.* **2000**, *113*, 10899 – 10912.
[12] K. Schmeide, T. Reich, S. Sachs, G. Bernhard, *Inorg. Chim. Acta* **2006**, *359*, 237 – 242.
[13] a) J. Wiebke, A. Morit, X. Cao, M. Dolg, *Phys. Chem. Chem. Phys.* **2007**, *9*, 459 – 465; b) A. Moritz, X. Y. Cao, M. Dolg, *Theor. Chem. Acc.* **2007**, *117*, 473 – 481.
[14] a) R. R. Pappalardo, E. Sánchez Marcos, *J. Phys. Chem.* **1993**, *97*, 4500 – 4504; b) J. M. Martínez, R. R. Pappalardo, E. Sánchez Marcos, *J. Am. Chem. Soc.* **1999**, *121*, 3175 – 3184; c) J. M. Martínez, F. Torrico, R. R. Pappalardo, E. Sánchez Marcos, *J. Phys. Chem. B* **2004**, *108*, 15851 – 15855.
[15] a) P. J. Merkling, A. Muñoz-Páez, J. M. Martínez, R. R. Pappalardo, E. Sánchez Marcos, *Phys. Rev. B* **2001**, *64*, 012201 – 4; b) P. J. Merkling, A. Muñoz-Páez, E. Sánchez Marcos, *J. Am. Chem. Soc.* **2002**, *124*, 10911 – 10920; c) P. D'Angelo, O. M. Roscioni, G. Chillemi, S. Della Longa, M. Benfatto, *J. Am. Chem. Soc.* **2006**, *128*, 1853 – 1858; d) F. Carrera, F. Torrico, D. T. Richens, A. Muñoz-Páez, J. M. Martínez, R. R. Pappalardo, E. Sánchez Marcos, *J. Phys. Chem. B* **2007**, *111*, 8223 – 8233.
[16] A. L. Ankudinov, A. I. Nesvizhskii, J. J. Rehr, *Phys. Rev. B* **2003**, *67*, 115120, and references therein.
[17] a) L. Helm, A. E. Merbach, *Chem. Rev.* **2005**, *105*, 1923 – 1960; b) M. Duvail, P. Vitorge, R. Spezia, *J. Chem. Phys.* **2009**, *130*, 104501; c) A. Villa, B. Hess, H. Saint-Martin, *J. Phys. Chem. B* **2009**, *113*, 7270 – 7281.

 © 2010 Wiley-VCH Verlag GmbH & Co. KGaA, Weinheim